

Published in final edited form as:

J Med Chem. 2012 July 26; 55(14): 6639–6643. doi:10.1021/jm300677j.

The Plant Growth Regulator Daminozide is a Selective Inhibitor of the Human KDM2/7 Histone Demethylases

Nathan R. Rose^{1,2,†}, Esther C.Y. Woon^{2,†,‡}, Anthony Tumber^{3,†}, Louise J. Walport², Rasheduzzaman Chowdhury², Xuan Shirley Li¹, Oliver N.F. King², Clarisse Lejeune^{2,3}, Stanley S. Ng^{3,4}, Tobias Krojer³, Mun Chiang Chan², Anna M. Rydzik², Richard J. Hopkinson², Ka Hing Che^{3,4}, Michelle Daniel³, Claire Strain-Damerell³, Carina Gileadi³, Grazyna Kochan³, Ivanhoe K. H. Leung², James Dunford⁴, Kar Kheng Yeoh⁵, Peter J. Ratcliffe⁵, Nicola Burgess-Brown³, Frank von Delft³, Susanne Muller³, Brian Marsden³, Paul E. Brennan³, Michael A. McDonough², Udo Oppermann^{3,4}, Robert J. Klose¹, Christopher J. Schofield^{2,*}, and Akane Kawamura^{2,*}

¹Epigenetic Regulation of Chromatin Function Group, Department of Biochemistry, University of Oxford, South Parks Road, Oxford, OX1 3QU U.K.

²Chemistry Research Laboratory, Department of Chemistry, University of Oxford, Mansfield Road, Oxford, OX1 3TA, U.K.

³Structural Genomics Consortium, University of Oxford, Headington OX3 7DQ, U.K.

⁴Botnar Research Centre, Oxford Biomedical Research Unit, Oxford OX3 7LD, U.K.

⁵Henry Wellcome Building for Molecular Physiology, Department of Clinical Medicine, University of Oxford, Roosevelt Drive, Oxford OX3 7BN, U.K.

Abstract

The JmjC oxygenases catalyse the *N*-demethylation of *N*^E-methyl lysine residues in histones and are current therapeutic targets. A set of 2-oxoglutarate analogues were screened using a unified assay platform for JmjC demethylases and related oxygenases. Results led to the finding that daminozide (*N*-(dimethylamino)succinamic acid, 160 Da), a plant growth regulator, selectively inhibits the KDM2/7 JmjC subfamily. Kinetic and crystallographic studies reveal daminozide chelates the active site metal via its hydrazide carbonyl and dimethylamino groups.

*Corresponding Authors: Dr. Akane Kawamura, Chemistry Research Laboratory, Department of Chemistry, University of Oxford, Mansfield Road, Oxford, OX1 3TA, U.K. akane.kawamura@chem.ox.ac.uk; Prof. Christopher J Schofield, Chemistry Research Laboratory, Department of Chemistry, University of Oxford, Mansfield Road, Oxford, OX1 3TA, U.K. christopher.schofield@chem.ox.ac.uk.

†Authors contributed equally to the work. This work involved contributions from multiple scientists and it is difficult to reflect relative contributions in terms of rank order in author lists.

‡Present Addresses

Dr. Esther C.Y. Woon, Department of Pharmacy, National University of Singapore, 18 Science Drive 4, Singapore 117543

Associated Content

Supporting Information Available: Assay methods, synthetic procedures, characterization of all synthesised compounds, ¹H NMR spectra of daminozide and analogues with iron(II), crystallographic data collection and refinement statistics. This material is provided free of charge via the Internet at <http://pubs.acs.org>. PDB ID Codes: 4AI9, 4AI8, 4DO0

Introduction

Histone modifications are central to the regulation of eukaryotic gene expression. The dynamic methylation of lysine and arginine residues in histones has diverse transcriptional outcomes, with different methylation sites and states being associated with promotion or repression of transcription. There are two classes of histone lysine demethylases (KDMs), the largest of which uses 2-oxoglutarate (2OG) as a cosubstrate (the JmjC enzymes) and comprises ~18 human enzymes grouped into 5 subfamilies (Figure 1). Several JmjC demethylases are targets for the treatment of diseases including leukaemia, breast and prostate cancers^{1,2} and inflammation.³ However, only limited inhibition data has been reported for the JmjC enzymes with few reports of selective inhibitors.⁴⁻⁸

2OG oxygenases have been targeted for therapeutic and agricultural applications⁹: an inhibitor of γ -butyrobetaine hydroxylase, BBOX1, is used clinically as a 'cardioprotectant', inhibition of the collagen prolyl hydroxylases has been investigated for treating fibrotic disease, and inhibitors of the hypoxia inducible factor hydroxylases are in clinical trials for the treatment of anaemia. These examples provide evidence that 2OG oxygenases are viable targets for therapeutic inhibition by small molecules in vivo. 2OG oxygenases involved in the biosynthesis of gibberellins, plant hormones involved in growth regulation, have also been targeted using small molecule inhibitors for both agricultural and horticultural applications. Here we report that daminozide, *N*-(Dimethylamino)succinamic acid, which was once widely used as a plant growth retardant but later withdrawn due to toxicity concerns, is a highly selective inhibitor of the KDM2/7 family of human JmjC histone demethylases.

Results

To enable the identification of selective JmjC demethylase subfamily inhibitors, we developed a unified screening platform containing representatives of each of the five human demethylase subfamilies (KDM2A/FBXL11, KDM3A/JMJD1A, KDM4E/JMJD2E, KDM5C/JARID1C, KDM6B/JMJD3) (Supporting Information). Active enzymes were expressed using bacterial or eukaryotic expression systems and purified to near homogeneity (Supporting Information). Kinetic parameters for 2OG and histone fragment substrates were determined (Table 1), and activity AlphaScreens (amplified luminescence proximity homogeneous assays) were developed (Figure S1).¹⁰ This assay is based on immunodetection of the lysine methylation state of biotin-conjugated histone peptide product, using Streptavidin- and Protein A- conjugated beads for quantification. For counter-screening, we selected three clinically relevant hypoxic response oxygenases, PHD2, FIH (prolyl and asparaginyl hydroxylases acting on Hypoxia Inducible Factor, respectively) and BBOX1 (γ -butyrobetaine hydroxylase) for which AlphaScreen or fluorescence assays¹¹ were also developed. This screening platform is a significant improvement on previous methods for human 2OG oxygenases⁹; it enables the oxygenases to be used at low nanomolar concentrations. Standardisation of the analytical methods for enzymes employing different types of substrates enabled quantitative comparisons of inhibitor potencies to be made.

In work aimed at identifying inhibitor scaffolds for the JmjC histone demethylases, we assembled a set of 2OG analogues known to inhibit 2OG oxygenases (Figure 2), and screened these against the 2OG oxygenase panel using the assay platform. As expected, known 'generic' 2OG oxygenase inhibitors⁹ including pyridine 2,4-dicarboxylic acid (compound **11**), and *N*-oxalylglycine (compound **12**) showed inhibition across the 2OG oxygenases tested, validating this assay platform. Interestingly, the clinically used histone deacetylase (HDAC) inhibitor Vorinostat/SAHA (suberoylanilide hydroxamic acid, compound **15**) inhibited several histone demethylases (Figure 2).

Unexpectedly, the plant growth regulator daminozide (compound **19**) stood out as a selective inhibitor of KDM2A ($IC_{50} = 1.5 \pm 0.7 \mu\text{M}$), which is selective for dimethyl lysine residues. Daminozide was identified as a plant growth retardant in the 1960s¹³ and used to control stem growth, plant size and fruit ripening for over 20 years.¹⁴ *In vivo*, daminozide is proposed to inhibit 2OG oxygenases involved in gibberellin, and possibly ethylene, biosynthesis in plants.^{15,16} However, daminozide usage in food crops was curtailed due to the potential carcinogenicity of its metabolite, 1,1-dimethylhydrazine (although is still used for ornamental plants).¹⁷⁻¹⁹ A formaldehyde dehydrogenase (FDH) coupled assay monitoring formaldehyde production confirmed the potency of daminozide against KDM2A ($IC_{50} = 1.5 \pm 0.4 \mu\text{M}$). To test further for subfamily selectivity, daminozide was screened against two other members of the KDM2/7 subfamily (PHF8 and KIAA1718, Table 1) which are structurally highly related to KDM2A and KDM2B, and are both also selective for demethylation of dimethyl lysine residues, but have different sequence specificities.²⁰⁻²² The results indicate that daminozide is at least 100-fold selective as an inhibitor of the KDM2/7 subfamily over the other demethylase subfamily members tested, with IC_{50} s of 2 μM or less against KDM2A, PHF8, and KIAA1718 and IC_{50} s of 127 μM for KDM3A (a different subfamily of dimethyl lysine demethylase) or greater (mM range) against other demethylases (Table 1). No inhibition was observed (at 1 mM) against other biologically important 2OG oxygenases that catalyse hydroxylation, i.e. PHD2, FIH and BBOX1. Given its simple achiral structure and low molecular weight (160 Da), the degree of selectivity exhibited by daminozide is remarkable.

Kinetic analyses revealed that daminozide is predominantly a competitive inhibitor with respect to 2OG ($K_i = 1.97 \mu\text{M}$) for KDM2A, but shows mixed inhibition with respect to peptide substrate, binding predominantly to the enzyme-peptide complex ($K_i = 85 \mu\text{M}$, $\alpha = 0.13$). (Figure 3). The latter observation is notable given that daminozide contains a dimethylamino group as do the KDM2/7 subfamily dimethyl lysine substrates, and might thus be expected to compete with the dimethylated lysine substrate. The pK_a of the daminozide hydrazide amine is 2.8, whilst that of its carboxylate is 4.6²³, suggesting that it may bind the active site iron; NMR analyses show daminozide complexes to Fe(II) in solution (Figure S2).

We then investigated the structural basis of the selective inhibition by daminozide on the KDM2/7 subfamily. We obtained structures of daminozide complexed with two demethylases, PHF8 and KDM4A, and a hydroxylase, FIH (Figure 4). The structures support the proposed general mode of inhibition by daminozide, i.e. by binding in the 2OG binding pocket and chelating to the active site metal via its acyl hydrazide carbonyl and

dimethylamino groups (Figure 4). Whilst the coordinate position of the daminozide carbonyl was invariant, i.e. in all cases *trans* to the Asp/Glu protein-based ligand, in the KDM4A structure the dimethylamino group was observed to complex either *trans* to His276 or *trans* to His188 in the two different molecules present in the asymmetric unit. Although in the case of PHF8 and FIH the daminozide dimethyl amino group was only observed to bind *trans* to the histidine equivalent to His276 of KDM4A, previous work²⁴ on complexes of 2OG oxygenases with 2OG and the cosubstrate analogue **12** demonstrate that the 1-carboxylate can bind in either of the two conformational positions, in an analogous manner to that observed for the dimethylamino group in the KDM4A structure. We propose that the selectivity of daminozide for the KDM2/7 subfamily could, at least in part, arise from a 'snug fit' obtained via binding in the position *trans* to His247 wherein its two methyl groups would be accommodated in a tight hydrophobic pocket (formed by Val255, Ile313, and Tyr257), which is conserved in the KDM2/7 subfamily (Figure 4). This pocket might bind the daminozide methyl groups less tightly in other demethylases/oxygenases because it is either more hydrophilic (as demonstrated by crystallographic analysis) or predicted to be more hydrophilic (by structure based on sequence alignments), for all the other 2OG oxygenases tested (Figure 1) (e.g. for KDM4A: Ser196, Thr270 and Asn198, KDM6B: Ser225, Ile291 and Asn227, FIH: Asn205, Ile273 and Phe257).

We also synthesised and tested analogues of daminozide (Table 1 and Table S3). The trimethylated analogue **22**, and compound **27**, both of which lack the terminal amine lone pair, displayed little/no KDM inhibition, consistent with the proposed mode of daminozide inhibition involving chelation by its terminal hydrazide amine. The monomethylated **23** and unmethylated analogues **24** were more potent than daminozide against KDM2A.

However, when tested against other 2OG subfamilies, these compounds were substantially less selective than daminozide (and were somewhat unstable in aqueous solution). The succinyl hydroxamic acid **25** and dioxoheptanoic acid **28**, in which the acyl-hydrazinamide of daminozide is replaced by metal-chelating hydroxamic acid and malonyl groups, respectively were also relatively potent but non-selective inhibitors (Table 1). Notably, compound **26**, in which the amide nitrogen of daminozide is *N*-methylated, is also selective for the KDM2/7 demethylases, albeit with reduced potency. Like daminozide, **26** has two methyl groups on the acyl hydrazide amine, suggesting that their presence confers selectivity. The other tested analogues were less active (Table S3).

Conclusions

Overall, we have demonstrated how the development of a screening platform employing multiple human 2OG oxygenases can enable the discovery of compounds selective for particular subfamilies. In the long term, we aim to help to develop screens for all human 2OG oxygenases and see them applied to the discovery of medicinally useful inhibitors. Using a relatively focused set of 2OG analogues, the screening platform led to the discovery that daminozide is a selective inhibitor of the KDM2/7 demethylase subfamily. Whilst daminozide itself is unlikely to be of medicinal use, the work has revealed a new class of 2OG oxygenase inhibitor, which employs alkylamino iron chelation. Of particular note is the high degree of selectivity exhibited by daminozide, especially given its achiral nature

and low molecular weight. The precise mode of action of daminozide as a plant growth regulator^{15,16}, and its potential human toxicity (if any) under physiologically relevant conditions are unknown. We have no evidence that our results are directly relevant to the toxicity issues relating to daminozide. However, the results do suggest a potential of daminozide or its derivatives to exert biological effects via the inhibition of 2OG oxygenases involved in epigenetics in animals and, potentially, in other organisms including plants. Given the link between JmjC enzymes and diseases including cancer^{2,3}, further work on the biological effects of daminozide are of interest.

Experimental Section

Chemical synthesis of potential inhibitors. Reagents and solvents were from Aldrich, Alfa Aesar or Acros. Reactions were monitored by TLC, which was performed on precoated aluminum-backed plates (Merck, silica 60 F254). Melting points were determined using a Leica Galen III hot-stage melting point apparatus and microscope. Infrared spectra were recorded from Nujol mulls between sodium chloride discs, on a Bruker Tensor 27 FT-IR spectrometer. NMR spectra were acquired using a Bruker DPX500 NMR spectrometer. Chemical shifts (δ) are given in ppm, and the multiplicities are given as singlet (s), doublet (d), triplet (t), quartet (q), multiplet (m), broad (br). Coupling constants J are given in Hz (± 0.5 Hz). High resolution mass spectra (HRMS) were recorded using a Bruker MicroTOF spectrometer. The purity of all compounds synthesized were 95% as determined by analytical reverse-phase HPLC (Ultimate 3000). Daminozide (AlarTM) and compound **28** are commercially available. The synthesis and characterisation of compounds **22**²⁵, **25**²⁶, **27**²⁷, **36**²⁸, **37**²⁹ and **38**²⁶ has been reported. The synthesis of compounds **31-35**, **39-41** and ¹³C NMR spectra for **22**, **23**, **24**, **26**, **31-35** are given in the Supporting Information.

4-(2,2,2-Trimethylhydrazinyl)-4-oxobutanoate **22**. The synthesis of compound **22** was as reported²⁵, thus reaction of daminozide (500mg, 3.1 mmol) with methyl iodide (700mg, 0.31 mL, 5.0 mmol) gave **22** as a white solid (75% yield), mp: 137-138 °C (lit. 1 137-138.5 °C); ¹H NMR (500 MHz, MeOD): δ 2.40 (t, $J = 6.5$ Hz, 2H), 2.51 (t, $J = 6.5$ Hz, 2H), 3.56 (s, 9H); ¹³C NMR (125 MHz, MeOD): δ 28.5, 29.1, 56.1, 170.4, 173.4; IR (neat) ν/cm^{-1} : 3405, 3312, 1729, 1693; HRMS (m/z): [M]⁺ calcd. for C₇H₁₅N₂O₃, 175.1077; found, 175.1081.

General procedure for the coupling of hydrazine to succinic anhydride. To a stirred solution of the appropriate hydrazine (1 equiv.) in acetonitrile (5 mL) was added dropwise a solution of succinic anhydride (200 mg, 2.0 mmol, 1 equiv.) in acetonitrile (5 mL). The mixture was stirred at room temperature for 24 h, after which the solvent was evaporated *in vacuo* and the resulting crude purified using semipreparative reverse-phase HPLC, performed on a phenomenex C18 column (150 mm \times 4.6 mm). Separation was achieved using a linear gradient of solvent A (water + 0.1% CF₃CO₂H) and solvent B (acetonitrile + 0.1% CF₃CO₂H), eluting at a flow rate of 1 mL/min and monitoring at 220 nm: 0% B to 40% B over 30 min.

4-(2-Methylhydrazinyl)-4-oxobutanoic acid **23**. Compound **23** is a colourless oil (63% yield), ¹H NMR (500 MHz, DMSO-d₆): δ 2.35 (t, $J = 7.0$ Hz, 2H), 2.68 (t, $J = 7.0$ Hz, 2H),

2.98 (s, 3H), 4.76 (s, 1H), 7.74 (s, 1H); ^{13}C NMR (125 MHz, DMSO- d_6): δ 28.3, 29.1, 170.1, 173.6; IR (neat) ν/cm^{-1} : 33 3219, 3057, 1708, 1632; HRMS (m/z): $[\text{M}+\text{Na}]^+$ calcd. for $\text{C}_5\text{H}_{10}\text{N}_2\text{NaO}_3$, 169.0584; found, 169.0577.

4-Hydrazinyl-4-oxobutanoic acid **24**. Compound 24 is a colourless oil (87% yield), ^1H NMR (500 MHz, DMSO- d_6): δ 2.34 (t, $J = 7.0$ Hz, 2H), 2.60 (t, $J = 7.0$ Hz, 2H), 5.86 (s, 1H), 8.99 (s, 1H); ^{13}C NMR (125 MHz, DMSO- d_6): δ 28.2, 29.1, 170.8, 173.9; IR (neat) ν/cm^{-1} : 3303, 3290, 3199, 1712, 1624; HRMS (m/z): $[\text{M}-\text{H}]^-$ calcd. for $\text{C}_4\text{H}_7\text{N}_2\text{O}_3$, 131.0462; found, 131.0468.

4-Oxo-4-(1,2,2-trimethylhydrazinyl)butanoic acid **26**. Compound 26 is a white solid (56% yield), mp: 97-98 °C, ^1H NMR (500 MHz, DMSO- d_6): δ 2.37 (t, $J = 7.0$ Hz, 2H), 2.66 (t, $J = 7.0$ Hz, 2H), 2.74 (s, 3H), 11.98 (s, 1H); ^{13}C NMR (125 MHz, DMSO- d_6): δ 28.2, 29.8, 43.4, 48.7, 173.5, 175.0; IR (neat) ν/cm^{-1} : 2958, 1723, 1615; HRMS (m/z): $[\text{M}+\text{Na}]^+$ calcd. for $\text{C}_7\text{H}_{14}\text{N}_2\text{NaO}_3$, 197.0897; found, 197.0895.

4-((Dimethylamino)oxy)-4-oxobutanoic acid **29**. *N,N*-Dimethylhydroxylamine (39 mg, 0.63 mmol, 1.1 equiv.) was added to a solution of 4-(tert-butoxy)-4-oxobutanoic acid (100 mg, 0.57 mmol, 1 equiv.), hydroxybenzotriazole (100 mg, 0.74 mmol, 1.3 equiv.), 1-ethyl-3-(3-dimethylaminopropyl) carbodiimide (140 mg, 0.74 mmol, 1.3 equiv.) and diisopropylethylamine (0.2 mL, 1.14 mmol, 2.0 equiv.) in CH_2Cl_2 (10 mL). The reaction was stirred at room temperature overnight, washed with water, HCl 1N, brine, dried on MgSO_4 . The organic phase was evaporated *in vacuo* and purified by chromatography (MeOH/ CH_2Cl_2 0.5/9.5) to obtain 110 mg of tert-butyl 4((dimethylamino)oxy)-4-oxobutanoate (90% yield). $\text{CF}_3\text{CO}_2\text{H}$ (0.04 ml, 0.37 mmol, 4 equiv.) was added to a solution of tert-butyl 4((dimethylamino)oxy)-4-oxobutanoate (20 mg, 0.09 mmol, 1 equiv.) in CH_2Cl_2 (1.5 ml). The reaction was stirred at room temperature for 4h and evaporated *in vacuo* to give 14 mg of 29 (yield 95%). ^1H NMR (500 MHz, CD_3OD) δ 2.59 (s, 6H), 2.57 (s, 4H); ^{13}C NMR (500 MHz, CD_3OD) δ 176.2, 172.0, 48.5, 29.9; IR (neat) 3341, 2485, 1717, 1120, 1026, 975 cm^{-1} ; HRMS (m/z): $[\text{M}^+]$ calcd. for $\text{C}_6\text{H}_{11}\text{NO}_4$ 161.0688; found 161.0923.

*N'*1, *N'*1, *N'*4, *N'*4-Tetramethylsuccinohydrazide **30**. A solution of succinic acid (100 mg, 0.85 mmol, 1 equiv.), hydroxybenzotriazole (350 mg, 2.11 mmol, 2.3 equiv.), 1-ethyl-3-(3-dimethylaminopropyl)carbodiimide (421 mg, 2.11 mmol, 2.3 equiv.), diisopropylethylamine (0.6 mL, 3.4 mmol, 4 equiv.) and 1,1-dimethylhydrazine (0.16 mL, 2.04 mmol, 2.2 equiv.) in CH_2Cl_2 (20 mL) was stirred at room temperature overnight. CH_2Cl_2 (10 mL) was added and the reaction mixture was washed with water, a saturated solution of NaHCO_3 , brine and dried on MgSO_4 . The organic phase was evaporated *in vacuo* and purified by chromatography (MeOH/ CH_2Cl_2 1/9) to give 77 mg of 30 (45% yield). ^1H NMR (500 MHz, CD_3OD) δ 2.87 (s, 6H), 2.65 (s, 2H); ^{13}C NMR (500 MHz, CD_3OD) δ 178.2, 43.8, 27.6; IR (neat) 3356, 2485, 2071, 1695, 1120, 1027, 974 cm^{-1} ; HRMS (m/z): $[(\text{M}-2\text{CH}_3)^-]$ calcd. for $\text{C}_6\text{H}_{14}\text{N}_4\text{O}_2$, 174.1117; found, 174.1022.

Supplementary Material

Refer to Web version on PubMed Central for supplementary material.

ACKNOWLEDGMENT

This research was supported in part by the The Wellcome Trust, The Commonwealth Scholarship Commission in the United Kingdom, the Biotechnology and Biological Research Council (U.K.) and the European Research Council. The Structural Genomics Consortium is a registered charity (number 1097737) that receives funds from the Canadian Institutes for Health Research, the Canadian Foundation for Innovation, Genome Canada through the Ontario Genomics Institute, GlaxoSmithKline, Karolinska Institutet, the Knut and Alice Wallenberg Foundation, the Ontario Innovation Trust, the Ontario Ministry for Research and Innovation, Merck & Co., Inc., the Novartis Research Foundation, the Swedish Agency for Innovation Systems, the Swedish Foundation for Strategic Research and the Wellcome Trust.

ABBREVIATIONS

2OG	2-oxoglutarate
BBOX	γ -butyrobetaine hydroxylase
FBXL	F-box, leucine-rich repeat protein
FIH	factor inhibiting hypoxia inducible factor
HDAC	histone deacetylase
JARID	jumonji, AT rich interactive domain containing protein
JmjC	jumonji-C domain
JMJD	jumonji-C domain containing protein
PHD2	human prolyl hydroxylase
PHF	plant homeodomain containing protein

REFERENCES

- (1). He J, Nguyen AT, Zhang Y. KDM2b/JHDM1b, an H3K36me2-specific demethylase, is required for initiation and maintenance of acute myeloid leukemia. *Blood*. 2011; 117(14):3869–3880. [PubMed: 21310926]
- (2). Yang J, Jubb AM, Pike L, Buffa FM, Turley H, Baban D, Leek R, Gatter KC, Ragoussis J, Harris AL. The histone demethylase JMJD2B is regulated by estrogen receptor alpha and hypoxia, and is a key mediator of estrogen induced growth. *Cancer Res*. 2010; 70(16):6456–6466. [PubMed: 20682797]
- (3). De Santa F, Totaro MG, Prosperini E, Notarbartolo S, Testa G, Natoli G. The Histone H3 Lysine-27 Demethylase Jmjd3 Links Inflammation to Inhibition of Polycomb-Mediated Gene Silencing. *Cell*. 2007; 130(6):1083–1094. [PubMed: 17825402]
- (4). Chang KH, King ON, Tumber A, Woon EC, Heightman TD, McDonough MA, Schofield CJ, Rose NR. Inhibition of histone demethylases by 4-carboxy-2,2'-bipyridyl compounds. *ChemMedChem*. 2011; 6(5):759–764. [PubMed: 21412984]
- (5). Hamada S, Suzuki T, Mino K, Koseki K, Oehme F, Flamme I, Ozasa H, Itoh Y, Ogasawara D, Komarashi H, Kato A, Tsumoto H, Nakagawa H, Hasegawa M, Sasaki R, Mizukami T, Miyata N. Design, synthesis, enzyme-inhibitory activity, and effect on human cancer cells of a novel series of jumonji domain-containing protein 2 histone demethylase inhibitors. *J Med Chem*. 2010; 53(15):5629–5638. [PubMed: 20684604]

- (6). Luo X, Liu Y, Kubicek S, Myllyharju J, Tumber A, Ng S, Che KH, Podoll J, Heightman TD, Oppermann U, Schreiber SL, Wang X. A selective inhibitor and probe of the cellular functions of Jumonji C domain-containing histone demethylases. *J Am Chem Soc.* 2011; 133(24):9451–9456. [PubMed: 21585201]
- (7). Rose NR, Ng SS, Mecinovic J, Liénard BMR, Bello SH, Sun Z, McDonough MA, Oppermann U, Schofield CJ. Inhibitor Scaffolds for 2-Oxoglutarate-Dependent Histone Lysine Demethylases. *J Med Chem.* 2008; 51(22):7053–7056. [PubMed: 18942826]
- (8). Sekirnik R, Rose NR, Mecinovic J, Schofield CJ. 2-Oxoglutarate oxygenases are inhibited by a range of transition metals. *Metallomics.* 2010; 2(6):397–399. [PubMed: 21072385]
- (9). Rose NR, McDonough MA, King ON, Kawamura A, Schofield CJ. Inhibition of 2-oxoglutarate dependent oxygenases. *Chem Soc Rev.* 2011; 40(8):4364–4397. [PubMed: 21390379]
- (10). Kawamura A, Tumber A, Rose NR, King ON, Daniel M, Oppermann U, Heightman TD, Schofield C. Development of homogeneous luminescence assays for histone demethylase catalysis and binding. *Anal Bioch.* 2010; 404(1):86–93. [PubMed: 20435012]
- (11). Rydzik A, Leung IKH, Kochan GT, Thalhammer A, Opperman U, Claridge TDW, Schofield CJ. Development and application of a fluoride detection based fluorescence assay for gamma-butyrobetaine hydroxylase. *ChemBioChem.* in press. [PubMed: 22730246]
- (12). Chowdhury R, Yeoh KK, Tian YM, Hillringhaus L, Bagg EA, Rose NR, Leung IKH, Li XS, Woon EC, Yang M, McDonough MA, King ON, Clifton IJ, Klose RJ, Claridge TDW, Ratcliffe PJ, Schofield CJ, Kawamura A. The oncometabolite 2-hydroxyglutarate inhibits histone lysine demethylases. *EMBO Rep.* 2011; 12(5):463–469. [PubMed: 21460794]
- (13). Riddell JA, Hageman HA, J'Anthony CM, Hubbard WL. Retardation of Plant Growth by a New Group of Chemicals. *Science.* 1962; 136(3514):391. [PubMed: 17798062]
- (14). Rademacher W. Growth Retardants: Effects on Gibberellin Biosynthesis and Other Metabolic Pathways. *Ann Rev Plant Physiol Plant Mol Biol.* 2000; 51(1):501–531. [PubMed: 15012200]
- (15). Brown RGS, Kawaide H, Yang Y-Y, Rademacher W, Kamiya Y. Daminozide and prohexadione have similar modes of action as inhibitors of the late stages of gibberellin metabolism. *Physiol Plant.* 1997; 101:309–313.
- (16). Looney NE. Inhibition of Apple Ripening by Succinic Acid, 2,2-Dimethyl Hydrazide and its Reversal by Ethylene. *Plant Physiol.* 1968; 43:1133–1137. [PubMed: 16656894]
- (17). Hasegawa R, Cabral R, Hoshiya T, Hakoi K, Ogiso T, Boonyaphiphat P, Shirai T, Ito N. Carcinogenic potential of some pesticides in a medium-term multi-organ bioassay in rats. *Int J Cancer.* 1993; 54(3):489–493. [PubMed: 8509224]
- (18). Mott L. Alar Again: Science, the Media, and the Public's Right to Know. *Int J Occup Environ Health.* 2000; 6(1):68–70. [PubMed: 10691344]
- (19). Toth B, Wallcave L, Patil K, Schmeltz I, Hoffmann D. Induction of tumors in mice with the herbicide succinic acid 2,2-dimethylhydrazide. *Cancer Res.* 1977; 37(10):3497–3500. [PubMed: 561652]
- (20). Horton JR, Upadhyay AK, Qi HH, Zhang X, Shi Y, Cheng X. Enzymatic and structural insights for substrate specificity of a family of jumonji histone lysine demethylases. *Nat Struct Mol Biol.* 2010; 17(1):38–43. [PubMed: 20023638]
- (21). Liu W, Tanasa B, Tyurina OV, Zhou TY, Gassmann R, Liu WT, Ohgi KA, Benner C, Garcia-Bassets I, Aggarwal AK, Desai A, Dorrestein PC, Glass CK, Rosenfeld MG. PHF8 mediates histone H4 lysine 20 demethylation events involved in cell cycle progression. *Nature.* 2010; 466(7305):508–512. 2010. [PubMed: 20622854]
- (22). Qi HH, Sarkissian M, Hu GQ, Wang Z, Bhattacharjee A, Gordon DB, Gonzales M, Lan F, Ongusaha PP, Huarte M, Yaghi NK, Lim H, Garcia BA, Brizuela L, Zhao K, Roberts TM, Shi Y. Histone H4K20/H3K9 demethylase PHF8 regulates zebrafish brain and craniofacial development. *Nature.* 2010; 466(7305):503–507. [PubMed: 20622853]
- (23). Schoenherr J, Bukovac MJ. Dissociation Constants of Succinic Acid 2,2-Dimethylhydrazide. *J Agr Food Chem.* 1972; 20(6):1263–1265.
- (24). Zhang Z, Ren J, Harlos K, McKinnon CH, Clifton IJ, Schofield CJ. Crystal structure of a clavamate synthase–Fe(II)–2-oxoglutarate–substrate–NO complex: evidence for metal centred rearrangements. *FEBS Letters.* 2002; 517(1–3):7–12. 2002. [PubMed: 12062399]

- (25). Wawzonek S, Kellen JN. Thermolysis of triethylamine with N-p-toluenesulfonylarylhidrazidoyl chlorides. *J Org Chem.* 1973; 38:2058–2061.
- (26). Mecinovic J, Loenarz C, Chowdhury R, Schofield CJ. 2-Oxoglutarate analogue inhibitors of prolyl hydroxylase domain 2. *Bioorg Med Chem Lett.* 2009; 19:6192–6195. [PubMed: 19775891]
- (27). Alain V, Dominique C, Frédéric Z, Roger L. Atypical Oxidation Reaction by Thionyl Chloride: Easy Two-Step Synthesis of N-Alkyl-1,4-dithiines. *Synthetic Commun.* 2006; 36:3591–3597.
- (28). Speiser, PP.; Joshi, RK. Fumaric acid derivatives, process for the production thereof and pharmaceutical compositions containing same. US 5149695 A. 1968.
- (29). Hageman, HA.; Hubbard, WL. N-disubstituted amino maleimides and succinimides. US 3257414 A. 1968.

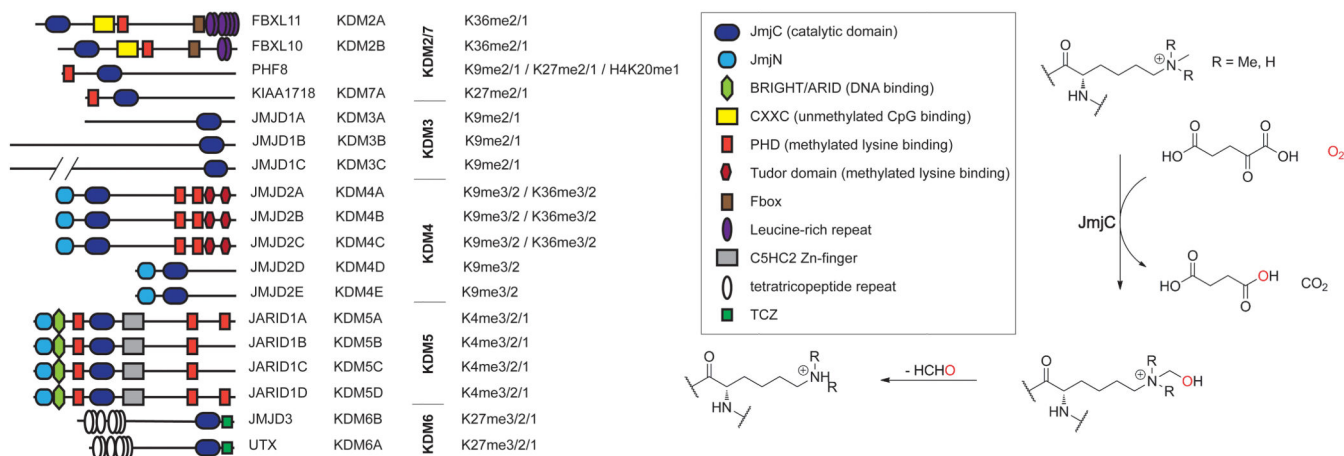


Figure 1. Subfamilies of the human 2-oxoglutarate ('JmjC') histone demethylases, showing their domain architecture

Not all proposed family members are shown. Each demethylation reaction is coupled to 2OG decarboxylation and formaldehyde production. KIAA1718 has recently been assigned as KDM7A, however its JmjC domain shows high sequence and structural similarity with the KDM2 subfamily members.

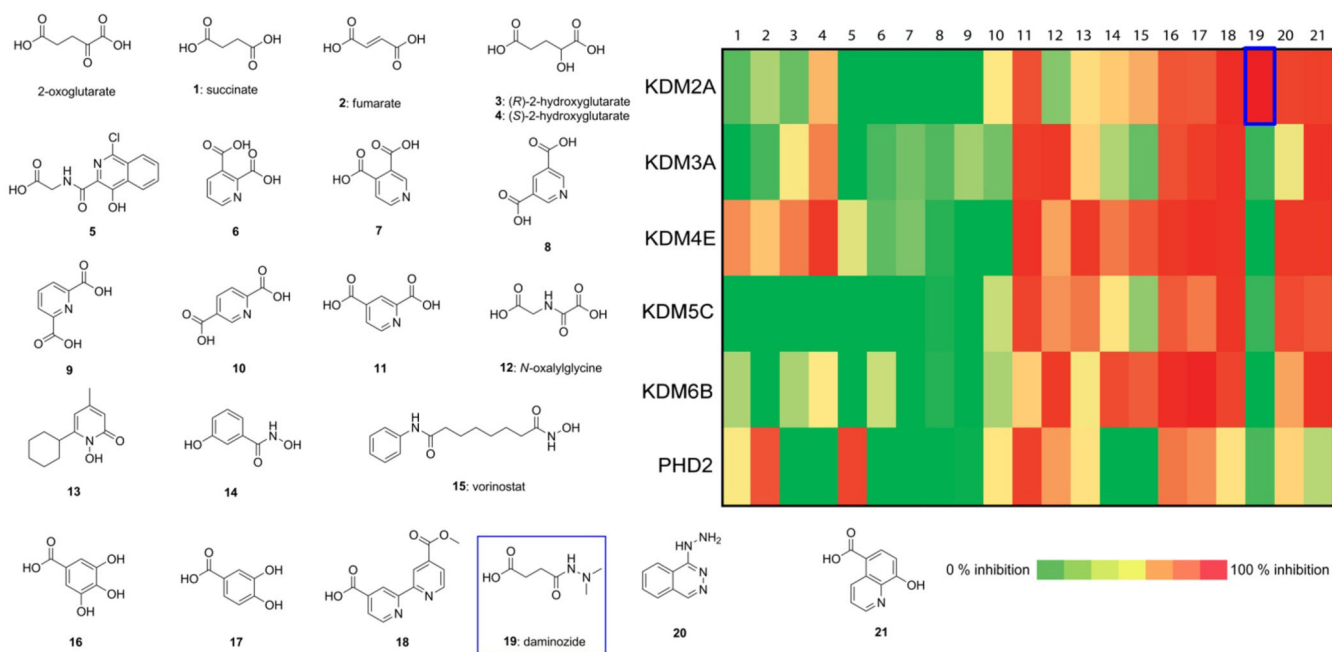


Figure 2. Heatmap of JmjC demethylase inhibition by a set of 20G analogues

Daminozide **19** is selective for KDM2A. Tricarboxylic acid cycle intermediates succinate **1** and fumarate **2** were generally poor demethylase inhibitors, though KDM4E⁷ was an exception to this trend. (*R*)- and (*S*)-2-hydroxyglutarate enantiomers, produced by gain-of-function mutations to isocitrate dehydrogenase were inhibitors of the KDM2, KDM3 and KDM4 histone demethylases.¹² The catechols **16** and **17**, bipyridyl **18** and 8-hydroxyquinoline **21** inhibited all demethylases screened. By contrast, **5** most potently inhibited PHD2 (prolyl hydroxylase domain enzyme isoform 2). Each compound was screened in an AlphaScreen assay and is represented as % inhibition of the enzyme at 20 μ M compound. Details of the assays are in the Supporting Information.

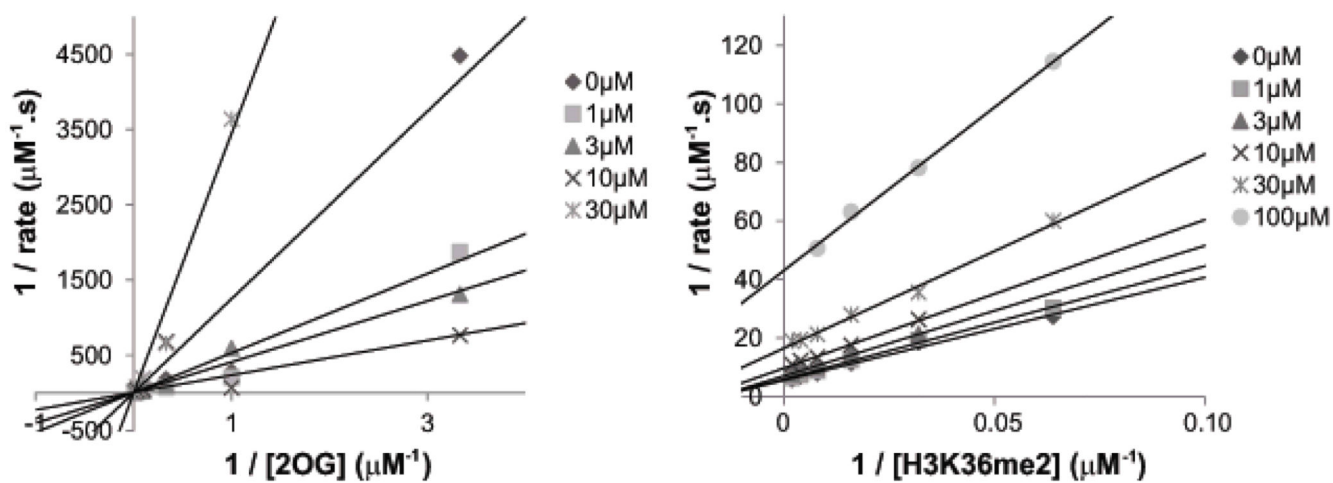


Figure 3. Mode of inhibition of the KDM2/7 subfamily by daminozide

Inhibition of KDM2A by daminozide is competitive with 2OG but not peptide substrate.

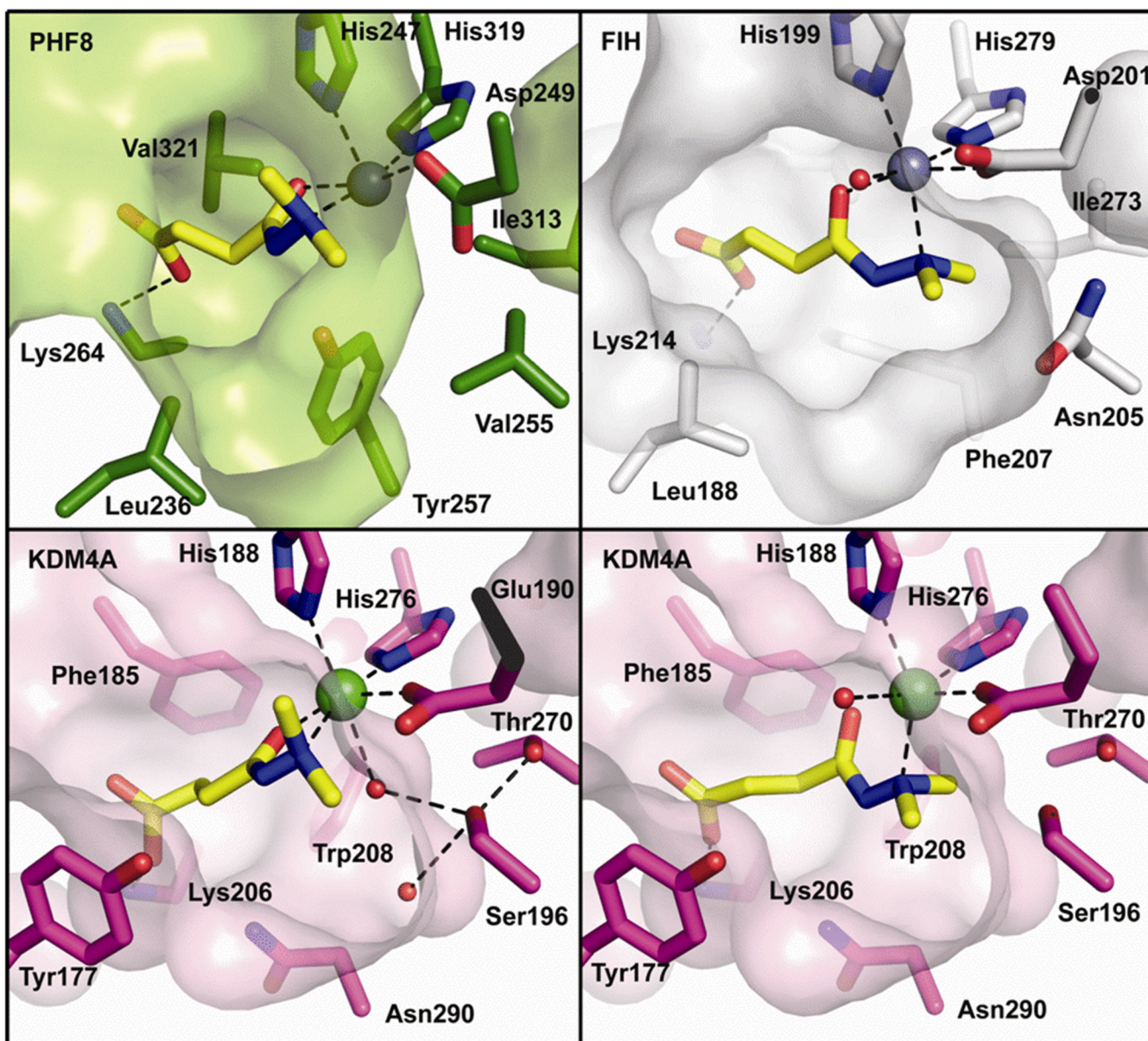


Figure 4. Crystal structures reveal the mode of inhibition of the KDM2/7 subfamily by daminozide
 PHF8 (with Zn(II) substituting for Fe(II),) and KDM4A (with Ni(II) substituting for Fe(II)) and FIH (with Zn(II) substituting for Fe(II)) (Table S3). Daminozide binds the metal through its hydrazide amine lone pair and carbonyl oxygen. Two distinct orientations of daminozide are observed in the two KDM4A molecules in the asymmetric unit; both are shown (see Table S2 for electron density maps). Selectivity of daminozide for the KDM2/7 subfamily may arise because they possess a hydrophobic region (Tyr257, Val255 and Ile313) into which the two daminozide methyl groups may bind. In contrast, the equivalent regions of KDM4A, FIH and the other tested demethylases/oxygenases are more hydrophilic.

Table 1
Inhibition data (IC₅₀) for daminozide and its analogues across KDMs and other 2OG oxygenases

Data are reported as IC₅₀ values in μM. AlphaScreen was used for all IC₅₀ determinations except where values are given in brackets where MALDI assay was used; all BBOX assays were run using a fluorescence based assay.¹¹ AlphaScreen assays were optimised to run at linear range of the reaction. Assays were performed at concentrations of 2OG near or below experimentally determined 2OG K_m values. Where K_m^{app} values for 2OG for enzymes were unknown, the kinetic parameter was determined by using the FDH assay: KDM2A (12.5 ± 1.4 μM), PHF8 (16.6 ± 1.8 μM), KDM3A (5.3 ± 2.2 μM), KDM5C (41.7 ± 6.3 μM) and KDM6B (5.4 ± 0.4 μM).

	Daminozide	22	23	24	25	26	27	28	29	30
KDM2A	1.5 ± 0.7	63	0.37	0.25	0.43	3.7	>100	0.57	9.1	>100
PHF8	0.55	35	3.4	0.48	1.7	11.5	>100	2.3	6.9	117
KIAA1718	(2.1)	-	-	-	-	-	-	-	-	-
KDM3A	>100	>100	>100	>100	3.0	>100	>100	12.7	>100	>100
KDM4E	>100	>100	4.3	0.2	0.4	>100	>100	23.9	>100	>100
KDM5C	>100	>100	1.1	0.48	1.9	>100	>100	4.5	42	>100
KDM6B	>100	>100	>100	>100	1.1	>100	>100	16.5	41.7	>100
FIH	(>100)	(>100)	(>100)	(>100)	(>100)	(>100)	(>100)	(>100)	(>100)	(>100)
PHD2	>100	>100	14.2	>100	19.6	>100	>100	>100	6.3	>100
BBOX1*	>100	>100	>100	>100	>100	>100	>100	>100	>100	>100